The Astrophysical Journal, 787:71 (6pp), 2014 May 20 doi:10.1088/0004-637X/787/1/71

OGLE-2012-BLG-0455/MOA-2012-BLG-206: MICROLENSING EVENT WITH AMBIGUITY IN PLANETARY INTERPRETATIONS CAUSED BY INCOMPLETE COVERAGE OF PLANETARY SIGNAL

H. Park[1], C. Han[1,25,26], A. Gould[2,26], A. Udalski[3,27], T. Sumi[4,28], P. Fouqué[5],
and
J.-Y. Choi[1], G. Christie[6], D. L. Depoy[7], Subo Dong[8], B. S. Gaudi[2], K.-H. Hwang[1], Y. K. Jung[1], A. Kavka[2], C.-U. Lee[9], L. A. G. Monard[10], T. Natusch[6,11], H. Ngan[6], R. W. Pogge[2], I.-G. Shin[1], J. C. Yee[2,12,29]
(The μFUN Collaboration)
M. K. Szymański[3], M. Kubiak[3], I. Soszyński[3], G. Pietrzyński[3,13], R. Poleski[3,2], K. Ulaczyk[3], P. Pietrukowicz[3], S. Kozłowski[3], J. Skowron[3], Ł. Wyrzykowski[3,14]
(The OGLE Collaboration)
F. Abe[15], D. P. Bennett[16], I. A. Bond[17], C. S. Botzler[18], P. Chote[19], M. Freeman[18], A. Fukui[20], D. Fukunaga[15], P. Harris[19], Y. Itow[15], N. Koshimoto[4], C. H. Ling[17], K. Masuda[15], Y. Matsubara[15], Y. Muraki[15], S. Namba[4], K. Ohnishi[21], N. J. Rattenbury[18], To. Saito[22], D. J. Sullivan[19], W. L. Sweatman[17], D. Suzuki[4], P. J. Tristram[23], K. Wada[4], N. Yamai[24], P. C. M. Yock[18], A. Yonehara[24]
(The MOA Collaboration)
[1] Department of Physics, Institute for Astrophysics, Chungbuk National University, Cheongju 371-763, Korea
[2] Department of Astronomy, The Ohio State University, 140 West 18th Avenue, Columbus, OH 43210, USA
[3] Warsaw University Observatory, Al. Ujazdowskie 4, 00-478 Warszawa, Poland
[4] Department of Earth and Space Science, Osaka University, Osaka 560-0043, Japan
[5] IRAP, CNRS, Université de Toulouse, F-31400 Toulouse, France
[6] Auckland Observatory, Auckland, New Zealand
[7] Department of Physics and Astronomy, Texas A&M University, College Station, TX 77843, USA
[8] Kavli Institute for Astronomy and Astrophysics, Peking University, Yi He Yuan Road 5, Hai Dian District, Beijing 100871, China
[9] Korea Astronomy and Space Science Institute, 776 Daedukdae-ro, Yuseong-gu, Daejeon 305-348, Korea
[10] Kleinkaroo Observatory, Calitzdorp, and Bronberg Observatory, Pretoria, South Africa
[11] Institute for Radiophysics and Space Research, AUT University, Auckland, New Zealand
[12] Harvard-Smithsonian Center for Astrophysics, 60 Garden Street, Cambridge, MA 02138, USA
[13] Departamento de Astronomia, Universidad de Concepción, Casilla 160-C, Concepción, Chile
[14] Institute of Astronomy, University of Cambridge, Madingley Road, Cambridge CB3 0HA, UK
[15] Solar-Terrestrial Environment Laboratory, Nagoya University, Nagoya 464-8601, Japan
[16] Department of Physics, University of Notre Dame, 225 Nieuwland Science Hall, Notre Dame, IN 46556-5670, USA
[17] Institute of Information and Mathematical Sciences, Massey University, Private Bag 102-904, North Shore Mail Centre, Auckland, New Zealand
[18] Department of Physics, University of Auckland, Private Bag 92-019, Auckland 1001, New Zealand
[19] School of Chemical and Physical Sciences, Victoria University, Wellington, New Zealand
[20] Okayama Astrophysical Observatory, National Astronomical Observatory of Japan, Asakuchi, Okayama 719-0232, Japan
[21] Nagano National College of Technology, Nagano 381-8550, Japan
[22] Tokyo Metropolitan College of Aeronautics, Tokyo 116-8523, Japan
[23] Mount John University Observatory, PO Box 56, Lake Tekapo 8770, New Zealand
[24] Department of Physics, Faculty of Science, Kyoto Sangyo University, 603-8555 Kyoto, Japan
Received 2014 March 7; accepted 2014 April 8; published 2014 May 5

ABSTRACT

Characterizing a microlensing planet is done by modeling an observed lensing light curve. In this process, it is often confronted that solutions of different lensing parameters result in similar light curves, causing difficulties in uniquely interpreting the lens system, and thus understanding the causes of different types of degeneracy is important. In this work, we show that incomplete coverage of a planetary perturbation can result in degenerate solutions even for events where the planetary signal is detected with a high level of statistical significance. We demonstrate the degeneracy for an actually observed event OGLE-2012-BLG-0455/MOA-2012-BLG-206. The peak of this high-magnification event ($A_{\rm max} \sim 400$) exhibits very strong deviation from a point-lens model with $\Delta\chi^2 \gtrsim 4000$ for data sets with a total of 6963 measurements. From detailed modeling of the light curve, we find that the deviation can be explained by four distinct solutions, i.e., two very different sets of solutions, each with a twofold degeneracy. While the twofold (so-called close/wide) degeneracy is well understood, the degeneracy between the radically different solutions is not previously known. The model light curves of this degeneracy differ substantially in the parts that were not covered by observation, indicating that the degeneracy is caused by the incomplete coverage of the perturbation. It is expected that the frequency of the degeneracy introduced in this work will be greatly reduced with the improvement of the current lensing survey and follow-up experiments and the advent of new surveys.

Key words: gravitational lensing: micro – planets and satellites: general

Online-only material: color figures

1. INTRODUCTION

Gravitational microlensing is one of the important methods to detect and characterize extrasolar planets. Due to its sensitivity to planets that are otherwise difficult to detect, the microlensing method is complementary to other methods. In particular, the method is sensitive to planets of low-mass stars located at or beyond the snow line, low-mass planets including terrestrial planets (Jung et al. 2014), and even free-floating planets (Sumi et al. 2011). For general review of planetary microlensing, see Gaudi (2012).

The microlensing signal of a planet is usually a short-term perturbation to the smooth and symmetric standard light curve of the primary-induced lensing event (Mao & Paczyński 1991; Gould & Loeb 1992). The planetary perturbation occurs when the source approaches planet-induced caustics, which represent the positions on the source plane at which the magnification of a point source would become infinite. For a lens composed of a star and a planet, caustics form a single or multiple sets of closed curves, each of which is composed of concave curves that meet at cusps. The number, size, and shape of caustics vary depending on the separation and the mass ratio between the planet and its host star. For a given planetary system, planetary perturbations further vary depending on how the source approaches the lens. As a result, planets exhibit very diverse signals in lensing light curves.

Due to the immense diversity of planetary signals, characterizing a microlensing planet is a difficult task. This characterization is done from modeling in which an observed lensing light curve is compared to numerous theoretical curves resulting from various combinations of the parameters describing the lens and the source. In this process, it is often confronted that solutions of different lensing parameters result in similar light curves and can explain the observed light curve. This degeneracy problem causes difficulty in the unique interpretation of the lens system. Therefore, understanding the causes of various types of degeneracy is very important.

Up to now, it is known that there exist three broad categories of degeneracy in the interpretation of planetary microlensing signals. The first category corresponds to the case for which the degeneracy occurs when different planetary systems induce similar caustics. Good examples are the "close/wide" degeneracy for binary-lens events (Griest & Safidazeh 1998; Dominik 1999; An 2005) and the "ecliptic" degeneracy for events affected by parallax effects (Skowron et al. 2011). The second category corresponds to the case for which the degeneracy occurs when light curves accidentally appear to be similar despite the fact that the caustics of the degenerate solutions are very different. Choi et al. (2012) presented two examples of events for which an observed perturbation could be interpreted by either a planetary or a binary companion. The third category corresponds to the case for which perturbations can be interpreted by solutions of totally different origins. A good example is the binary-lens/binary-source degeneracy (Gaudi 1998; Gaudi & Han 2004; Hwang et al. 2013).

In this work, we show that incomplete coverage of a perturbation can also result in degenerate solutions even for events where the planetary signal is detected with a high level of statistical significance. We demonstrate the degeneracy for an actually observed event OGLE-2012-BLG-0455/MOA-2012-BLG-206.

2. OBSERVATION

The microlensing event OGLE-2012-BLG-0455/MOA-2012-BLG-206 occurred on a star located close to the Galactic center with equatorial coordinates $(\alpha, \delta)_{J2000} = (17^h51^m32^s.42, -28^\circ33'42''.3)$, corresponding to the Galactic coordinates $(l, b) = (0^\circ.99, -0^\circ.92)$. The lensing-induced brightening of the source star was first noticed on 2012 April 16 from the lensing survey conducted by the Optical Gravitational Lensing Experiment (OGLE: Udalski 2003) using the 1.3 m Warsaw telescope of Las Campanas Observatory in Chile. The event was independently detected from the survey done by the Microlensing Observations in Astrophysics (MOA: Bond et al. 2001; Sumi et al. 2003) group using the 1.8 m telescope of Mount John Observatory in New Zealand. Based on real-time modeling of OGLE and MOA data (posted on their Web sites[30,31]), the Microlensing Follow-Up Network (μFUN: Gould et al. 2006) issued a second-level alert just 9 hr before the peak, predicting that the event would be very high magnification ($A_{max} > 300$) and so would be extremely sensitive to planets (Griest & Safidazeh 1998). In response to the high-magnification alert, data were taken first by using the 0.36 m telescope of Kleinkaroo Observatory (KKO) in South Africa and subsequently by using the 1.3 m SMARTS telescope of Cerro Tololo Inter-American Observatory (CTIO) in Chile and the 0.4 m telescope of Auckland Observatory in New Zealand. From follow-up observations, the peak of the event was densely covered, especially by the CTIO data, which are composed of 55 images in I, 8 images in V, and 295 images in H band. The total number of measurements is 6963. However, the coverage is not complete because the event occurred during the early bulge season when the duration of Galactic-bulge visibility was short and follow-up observation in other parts of the Earth was not fully operational.

The OGLE and MOA data were reduced using photometry codes developed by the individual groups, based on the difference image analysis technique (Alard & Lupton 1998; Woźniak et al. 2000; Bond et al. 2001). The μFUN data were initially reduced by the DoPHOT pipeline (Schechter et al. 1993) and were reprocessed using the pySIS package (Albrow et al. 2009) to refine the photometry. Photometric errors estimated by different photometry systems may vary. Furthermore, error bars of each data set may deviate from the dispersion of the data points due to systematics in the photometry system. In order to use data sets collected from different observatories, we therefore normalize error bars. For this, we first add a quadratic term so that the cumulative distribution of χ^2 ordered by magnification is approximately linear to ensure that the dispersion of the data points is consistent with error bars regardless of the source brightness. We then rescale the errors so that χ^2 per degree of freedom (χ^2/dof) for each data set becomes unity to ensure that each data set is fairly weighted according to error bars.

In Figure 1 we present the light curve of the event. The event reached a magnification $A_{max} \sim 400$ at the peak.[32] At a glance, the light curve appears to have a standard form of an event caused by a point mass. However, a single-lens fit leaves significant

[25] Author to whom any correspondence should be addressed.
[26] The μFUN Collaboration.
[27] The OGLE Collaboration.
[28] The MOA Collaboration.
[29] Sagan Fellow.

[30] http://ogle.astrouw.edu.pl
[31] http://www.phys.canterbury.ac.nz/moa
[32] We note that the apparent lensing magnification $A_{obs} \sim 35$, corresponding to the magnitude change ~3.5 mag, is much smaller than the measured magnification $A_{max} \sim 400$, because the lensed star is heavily blended with other neighboring stars.

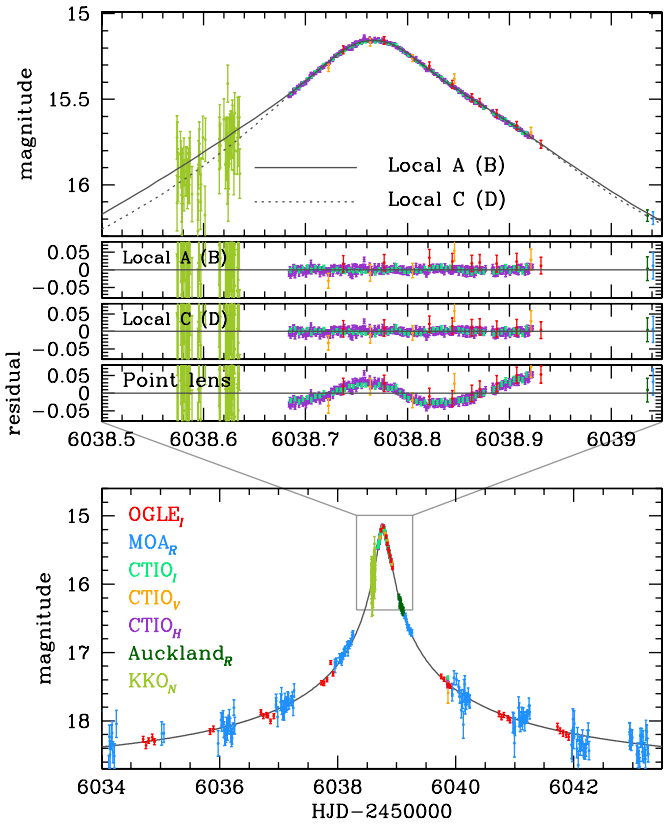

Figure 1. Light curve of OGLE-2012-BLG-0455/MOA-2012-BLG-206. In the legends indicating observatories, the subscript of each observatory denotes the passband. The top panels show the zoom of the peak region, where solid and dotted curves represent the models of the degenerate solutions. The three middle panels show the residuals from the two degenerate planetary solutions and the point-lens model.

(A color version of this figure is available in the online journal.)

residual near the peak. Such a deviation at the peak is typically produced by either a planetary or a binary companion to the primary lens.

3. MODELING

Keeping the possible cause of the perturbation in mind, we analyze the light curve based on two-point-mass lens modeling. Basic description of a binary-lens event requires seven parameters. Among them, the first three describe the lens-source approach, including the time of the closest approach of the source to a reference position of the binary lens, t_0, the lens-source separation at t_0 in units of the angular Einstein radius $\theta_{\rm E}$ of the lens, u_0, and the time required for the source to cross the Einstein radius, $t_{\rm E}$ (Einstein timescale). Another three parameters describe the two-point lens, including the projected binary separation in units of the Einstein radius, s, the mass ratio between the lens components, q, and the angle between the source trajectory and the binary axis, α. The last parameter is the ratio of the angular source radius θ_* to the Einstein radius, $\rho_* = \theta_*/\theta_{\rm E}$ (normalized source radius), which is needed to describe the effect of the extended source on the light curve.

Besides the basic lensing parameters, additional parameters are often needed to describe subtle deviations of lensing light curves caused by second-order effects. One such effect is the orbital motion of a binary lens, which induces variation of the caustic shape during the magnification phase (Albrow et al. 2000; An et al. 2002; Penny et al. 2011; Shin et al. 2011; Park et al. 2013). Another effect is caused by the orbital motion of the Earth, which results in deviation of the source motion from rectilinear (Gould 1992). The latter effect is often referred to as a parallax effect. We find that these effects are not important for OGLE-2012-BLG-0455/MOA-2012-BLG-206 mainly because of the relatively short duration of the event and moderate photometric quality in the wing and baseline.

The search for the best-fit solution of the lensing parameter is conducted in two steps. In the first step, we conduct a grid search in the (s, q, α) parameter space in order to locate all possible local minima. In this process, the remaining parameters $(t_0, u_0, t_{\rm E}, \rho_*)$ are searched by a downhill approach to yield minimum χ^2 at each grid point. In the second step, we investigate the individual local minima found from the initial search. At this stage, we refine each local minimum by allowing all parameters to vary. For χ^2 minimization, we use the Markov chain Monte Carlo (MCMC) method.

We compute finite-source magnifications by using the inverse ray-shooting method. In this numerical method, uniform rays are shot from the image plane, bent by the lens equation, and arrive at the source plane. We note that the term "inverse" is used to denote that rays are traced *backward* from the image plane to the source plane. Then, the magnification affected by the extended source is computed as the ratio between the number densities of rays on the source surface and on the image plane (Schneider & Weiss 1986; Kayser et al. 1986; Wambsganss 1997). The lens equation of a binary lens is expressed as

$$\zeta = z - \sum_{i=1}^{2} \frac{\epsilon_i}{\overline{z} - \overline{z}_{{\rm L},i}}, \quad (1)$$

where ζ, $z_{{\rm L},i}$, and z represent the complex notations of the source, lens, and image positions, respectively, the overbar denotes complex conjugate, ϵ_i are the mass fractions of the lens components, and the index $i = 1, 2$ denotes the individual lens components. In computing finite magnifications, we consider the limb-darkening effect of the source star by modeling the surface brightness profile as

$$S_\lambda \propto 1 - \Gamma_\lambda \left(1 - \frac{3}{2}\cos\psi\right), \quad (2)$$

where Γ_λ is the linear limb-darkening coefficient, λ is the passband, and ψ is the angle between the line of sight toward the source star and the normal to the source surface. The limb-darkening coefficients are adopted from Claret (2000) considering the source type estimated based on the location in the color–magnitude diagram. It is estimated that the source type is an F-type main-sequence star with the dereddened color $(V - I)_0 = 0.60$ and I magnitude $I_0 = 18.6$. Based on the source type, we adopt the coefficients $\Gamma_V = 0.497$, $\Gamma_R = 0.421$, $\Gamma_I = 0.347$, and $\Gamma_H = 0.199$. For the MOA data, which used a nonstandard filter system, we choose a mean value of the R- and I-band coefficients, i.e., $(\Gamma_R + \Gamma_I)/2$.

4. RESULTS

From detailed analysis of the light curve, we find that the light curve significantly deviates from a standard point-mass model with $\Delta\chi^2 \gtrsim 4000$. However, despite such a strong signal, interpreting the deviation is difficult due to the existence of very degenerate local minima in the parameter space. Figure 2 shows the local minima presented as a $\Delta\chi^2$ distribution in the (s, q)

Table 1
Lensing Parameters of Four Degenerate Solutions

Parameters	Local A	Local B	Local C	Local D
χ^2/dof	6963.6/6956	6962.7/6956	6957.6/6956	6957.7/6956
t_0 (HJD-2450000)	6038.7683 ± 0.0004	6038.7689 ± 0.0004	6038.7768 ± 0.0005	6038.7770 ± 0.0005
u_0 (10^{-3})	2.32 ± 0.17	2.21 ± 0.10	2.14 ± 0.12	2.23 ± 0.17
t_E (days)	47.4 ± 3.3	50.3 ± 2.3	50.1 ± 2.6	48.0 ± 3.6
s	0.23 ± 0.02	4.99 ± 0.39	0.77 ± 0.02	1.33 ± 0.04
q (10^{-3})	9.55 ± 2.26	11.30 ± 1.74	0.07 ± 0.01	0.08 ± 0.01
α (rad)	4.777 ± 0.009	4.782 ± 0.009	4.209 ± 0.003	4.211 ± 0.004
ρ_* (10^{-3})	1.56 ± 0.12	1.35 ± 0.09	1.08 ± 0.06	1.11 ± 0.09

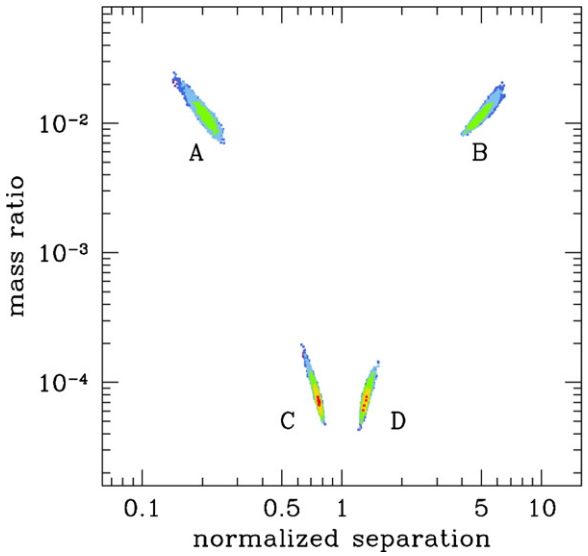

Figure 2. Distribution of $\Delta\chi^2$ in the parameter space of the normalized projected separation s and the mass ratio q. Different contours correspond to $\Delta\chi^2 < 1$ (red), 4 (yellow), 9 (green), 16 (light blue), 25 (blue), and 36 (purple), respectively.

(A color version of this figure is available in the online journal.)

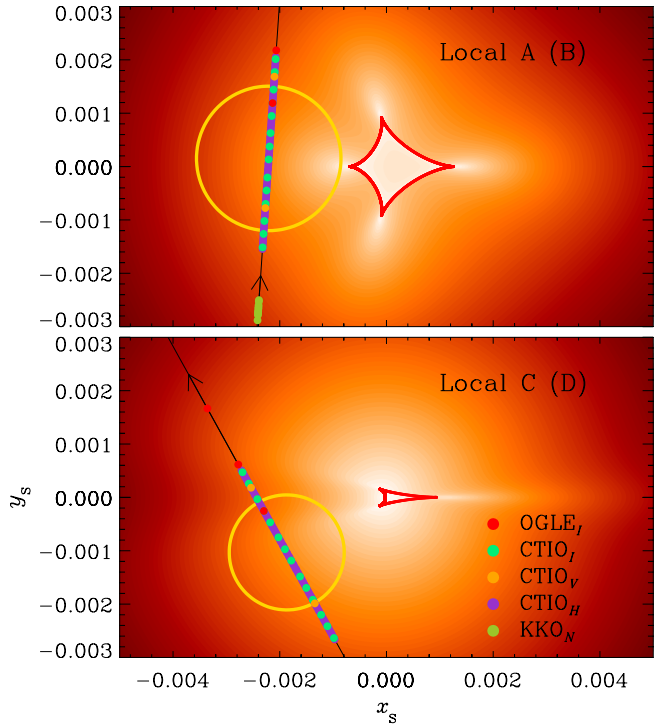

Figure 3. Geometries and magnification patterns for the best-fit models of Local A or B (upper panel) and C or D (lower panel). The brighter tone denotes higher magnifications. The closed red curves represent the caustics. In each panel, the straight line with an arrow represents the source trajectory. The size of the empty yellow circle represents the source size. The dots on the trajectories represent the source positions at the times when data were taken.

(A color version of this figure is available in the online journal.)

parameter space. It is found that four distinct local minima exist. We mark the individual minima as A, B, C, and D. In Table 1, we list the lensing parameters of the individual local minima. We note that the mass ratios of all the minima are less than 10^{-2}, implying that the companion is in the planetary mass regime. However, the degeneracy among the local solutions is very severe with $\Delta\chi^2 \lesssim 5$ for dof $= 6956$[33] and thus the characteristics of the planet cannot be uniquely determined.

Among the local solutions, the degeneracies between the A–B and C–D pairs are already known. For each of these pairs, the mass ratios are similar, but the projected separations have opposites signs of $\log s$, i.e., $s \leftrightarrow s^{-1}$. For such pairs of binary lenses, the caustics located near the primary lens induced by the close ($s < 1$) and wide ($s > 1$) planetary companions are similar in both size and shape, causing degeneracy in the resulting light curve. This degeneracy, known as the close/wide degeneracy, is caused by the invariance of the caustic under the $s \leftrightarrow s^{-1}$ transformation (Griest & Safizadeh 1998; Dominik 1999; An 2005; Chung et al. 2005).

On the other hand, the degeneracies between the A-C and B-D pairs are not previously known. For each of these pairs, the lens systems of the individual local solutions have widely different characteristics. For example, the values of the separation and mass ratio are $(s, q) = (0.23, 9.50 \times 10^{-3})$ for the local solution "A," while the values are $(s, q) = (0.77, 0.07 \times 10^{-3})$ for the solution "C." Based on the mass ratio, the individual solutions imply that the planet is either a super-Jupiter or a Neptune-mass planet if the primary is a normal star. Due to the wide difference in the planet parameters, the caustics and the magnification patterns around the caustics of the degenerate solutions are greatly different as shown in Figure 3. Despite the difference in caustics, we find that the two solutions are very degenerate with $\Delta\chi^2 \lesssim 5$.

Although the former degeneracy is severe because it is intrinsically rooted in the lens equation, the latter degeneracy results from widely different lens systems, and thus it might be that the degeneracy could be resolved with additional information. We therefore conduct three additional tests to check the feasibility of resolving the degeneracy.

The first test is to compare limb-darkening effects of the source star. For the high mass ratio solutions (local A and B),

[33] We note that the source star of the event had been observed since 2010, and thus there exist many more data points not shown in Figure 1.

the source approaches the caustic close enough for the edge of the source star to almost touch the caustic. For the low mass ratio solutions (local C and D), on the other hand, the source-caustic separation is relatively wide. Then, the limb-darkening effect would be more important for the high mass ratio solution than the low mass ratio solution. We investigate the limb-darkening effect by measuring the color variation in the CTIO *I* and *H* data taken during the caustic approach. Unfortunately, the expected color variation from the models is substantially smaller than the photometric errors. Therefore, this method cannot be applied to resolve the degeneracy.

The second test is to compare source fluxes estimated from the degenerate solutions. If they are different, high-resolution imaging from either space-based or ground-based adaptive optics observations would enable one to distinguish the solutions by resolving blended stars. However, we find that the source and blend fluxes for the two locals are nearly identical, and thus the method cannot be applied to resolve the degeneracy, either.

The third test is to compare the relative lens-source proper motions μ of the two degenerate solutions. If they differ by an amount substantially greater than the measurement error, it would be possible to resolve the degeneracy from future follow-up observation by using high-resolution space- or ground-based instruments. We estimate the proper motions by $\mu = \theta_{\rm E}/t_{\rm E}$, where the Einstein timescale $t_{\rm E}$ is measured from light-curve modeling and the angular Einstein radius $\theta_{\rm E}$ is estimated from the angular source radius θ_* and the normalized source radius ρ_* by $\theta_{\rm E} = \theta_*/\rho_*$. The angular source radius is estimated based on the dereddened color and brightness of the source. The measured values are $\mu = 2.91 \pm 0.27$ (0.16) mas yr^{-1} for the high mass ratio solution and $\mu = 3.68 \pm 0.30$ (0.15) mas yr^{-1} for the low mass ratio solution. We present two sets of errors where one (in the parentheses) is estimated just based on the MCMC chain of the solution, while the other value is estimated by adding an additional 7% error in quadrature to account for errors accompanied in the color-to-θ_* conversion process. The fractional error of the proper-motion difference is $\sigma_{\Delta\mu}/\Delta\mu \sim 50\%$ (28%). Considering the large fractional error, it would not be easy to resolve the degeneracy by using this method.

Although very degenerate with the current data, however, we find that the latter degeneracy could have been resolved if the perturbation had been continuously and precisely covered by additional data. This can be seen in the model light curves of the two degenerate solutions presented in Figure 1 (solid curve for the high mass ratio solution and dotted curve for the low mass ratio solution). It is found that the difference between the two model light curves in the region $6038.27 \lesssim {\rm HJD} - 2{,}450{,}000 \lesssim 6038.68$ is considerable, with a maximum magnitude difference reaching ~0.08 mag. Although a portion of this region $6038.56 \lesssim {\rm HJD} - 2{,}450{,}000 \lesssim 6038.64$ was covered by the KKO data, the event was still quite faint given the smaller aperture (36 cm) of the telescope, and thus the signal-to-noise ratio was not high enough to distinguish between models. Considering that photometric errors of adjacent data taken by 1 m class telescopes are ~0.01 mag, the degeneracy could have been easily resolved if the perturbation had been continuously covered by mid-size telescopes. Therefore, the degeneracy can be attributed to the incomplete coverage of the planetary perturbation. Considering this, the degeneracy is different from the case where degenerate light curves are alike in all parts.

5. CONCLUSION

We analyzed the high-magnification microlensing event OGLE-2012-BLG-0455/MOA-2012-BLG-206 for which the peak of the light curve exhibited an anomaly. Despite a large deviation from a standard point-mass model, it was found that four very degenerate local solutions existed. While two of these were due to the well-known $s \leftrightarrow s^{-1}$ "close/wide" degeneracy, the other degeneracy, between high and low mass ratios q, was previously unknown. From the fact that the model light curves of the latter degeneracy substantially differed in the parts that were not covered by observation, it was found that the degeneracy was caused by the incomplete coverage of the perturbation. Therefore, the event illustrated the importance of continuous coverage of perturbations for accurate determinations of lens properties.

It is expected that the frequency of the degeneracy introduced in this work will be greatly reduced with the improvement of lensing surveys. Recently, there has been such improvement for the existing lensing surveys. For example, the observation cadence of the OGLE lensing survey was substantially increased with the adoption of a new wide-field camera. The recent joining of the Wise survey (Shvartzvald et al. 2014) being conducted in Israel enables more continuous event coverage by filling the gap between telescopes in Oceania and Chile. Furthermore, there are plans for future lensing surveys. For example, the MOA group plans to additionally locate a new telescope in Africa for better coverage of lensing events. In addition, the Korea Microlensing Telescope Network (KMTNet) will start operation from the 2014 season by using a network of telescopes at three different locations in the Southern Hemisphere (Chile, South Africa, and Australia). The KMTNet project plans to achieve 10-minute cadence. In addition to survey experiments, there also has been important progress in follow-up experiments. The most important is the completion of the Las Cumbres Observatory Global Telescope Network, which is an integrated set of robotic telescopes distributed around the world, including two 2 m telescopes in Hawaii and Australia and nine 1 m telescopes sited in Chile, South Africa, Australia, and Texas (Tsapras et al. 2009). With the expansion of both survey and follow-up experiments, round-the-clock coverage of lensing events will be possible and the occurrence of the degeneracy will be greatly decreased.

Work by C.H. was supported by the Creative Research Initiative Program (2009-0081561) of the National Research Foundation of Korea. A.G. and B.S.G. acknowledge support from NSF AST-1103471. B.S.G., A.G., and R.W.P. acknowledge support from NASA grant NNX12AB99G. The OGLE project has received funding from the European Research Council under the European Community's Seventh Framework Programme (FP7/2007-2013)/ERC grant agreement No. 246678 to A.U. The MOA experiment was supported by grants JSPS22403003 and JSPS23340064. T.S. acknowledges the support from the grant JSPS24253004. T.S. is supported by the grant JSPS23340044. Y.M. acknowledges support from JSPS grants JSPS23540339 and JSPS19340058. S.D. was supported through a Ralph E. and Doris M. Hansmann Membership at the IAS and NSF grant AST-0807444. Work by J.C.Y. was performed in part under contract with the California Institute of Technology (Caltech) funded by NASA through the Sagan Fellowship Program.

REFERENCES

Alard, C., & Lupton, R. H. 1998, ApJ, 503, 325
Albrow, M. D., Beaulieu, J.-P., Caldwell, J. A. R., et al. 2000, ApJ, 534, 894
Albrow, M. D., Horne, K., Bramich, D. M., et al. 2009, MNRAS, 397, 2099
An, J. H., Albrow, M. D., Beaulieu, J. P., et al. 2002, ApJ, 572, 521
Bond, I. A., Abe, F., Dodd, R. J., et al. 2001, MNRAS, 327, 868
Claret, A. 2000, A&A, 363, 1081
Choi, J.-Y., Shin, I.-G., Han, C., et al. 2012, ApJ, 756, 48
Chung, S.-J., Han, C., Park, B.-G., et al. 2005, ApJ, 630, 535
Dominik, M. 1999, A&A, 349, 108
Gaudi, B. S. 1998, ApJ, 506, 533
Gaudi, B. S. 2012, ARA&A, 50, 411
Gaudi, B. S., & Han, C. 2004, ApJ, 611, 528
Gould, A. 1992, ApJ, 392, 442
Gould, A., & Loeb, A. 1992, ApJ, 396, 104
Gould, A., Udalski, A., An, D., et al. 2006, ApJ, 644, 37
Griest, K., & Safizadeh, N. 1998, ApJ, 500, 37
Hwang, K.-H., Choi, J.-Y., Bond, I. A., et al. 2013, ApJ, 778, 55
Jung, Y. K., Park, H., Han, C., et al. 2014, ApJ, 786, 85
Kayser, R., Refsdal, S., & Stabell, R. 1986, A&A, 166, 36
Mao, S., & Paczyński, B. 1991, ApJL, 374, L37
Park, H., Udalski, A., Han, C., et al. 2013, ApJ, 778, 134
Penny, M. T., Mao, S., & Kerins, E. 2011, MNRAS, 412, 607
Schechter, P. L., Mateo, M., & Saha, A. 1993, PASP, 105, 1342
Schneider, P., & Weiss, A. 1986, A&A, 164, 237
Shin, I.-G., Udalski, A., Han, C., et al. 2011, ApJ, 735, 85
Shvartzvald, Y., Maoz, D., Kaspi, S., et al. 2014, MNRAS, 439, 604
Skowron, J., Udalski, A., Gould, A., et al. 2011, ApJ, 738, 87
Sumi, T., Abe, F., Bond, I. A., et al. 2003, ApJ, 591, 204
Sumi, T., Kamiya, K., Bennett, D. P., et al. 2011, Natur, 473, 349
Tsapras, Y., Street, R., Horne, K., et al. 2009, AN, 330, 4
Udalski, A. 2003, AcA, 53, 291
Wambsganss, J. 1997, MNRAS, 284, 172
Woźniak, P. R. 2000, AcA, 50, 421